Position Control for Automatic Assembly Equipment Using a New Hybrid Fuzzy Controller

Longjie Zhang[1], Mingxia Kang[1], Xinhua Liu[1,*], Zhixiong Li[2]
[1]Department of Mechatronics Engineering, China University of Mining and Technology, University Rd. 1, 211006 Xuzhou, China
[2]Faculty of Mechanical Engineering, Opole University of Technology, ul. Proszkowska 76, 45-758 Opole, Poland
*ts22050209p31@cumt.edu.cn; 6174@cumt.edu.cn; *liuxinhua@cumt.edu.cn; z.li@po.edu.pl*

***Abstract*—Automatic assembly equipment is the key to improving the efficiency and quality of workpiece assembly. The precision of assembly directly influences the overall quality of the assembled product. To optimise the position control accuracy in the automatic assembly equipment, a variable universe fuzzy proportional integral (VUFPI) controller optimised by the sparrow search algorithm (SSA) is developed in this paper. The developed controller adopts the SSA to adjust in real time the universe of the fuzzy controller according to the deviation of the servo system. The servo system model is established to evaluate the performance of the proposed SSA-VUFPI controller; furthermore, the SSA-VUFPI controller is implemented in the automatic assembly equipment for experimental evaluation. The analysis results demonstrate that the proposed SSA-VUFPI controller is capable of improving the anti-interference ability and position accuracy of the servo system compared to traditional PI, VUFPI, and currently used back propagation neural network proportional-integral-derivative (BP-PID), fractional-order PID (FOPID), and SSA-PID controllers. Moreover, it effectively improves the position accuracy of the workpiece and ultimately improves the quality of the assembly.**

***Index Terms*—Automatic assembly equipment; Fuzzy control; Position control.**

I. INTRODUCTION

Assembly is a key process in modern mechanical products, which significantly influences product performance, quality, development timelines, and costs. Over the past few decades, automatic assembly has been a challenging research area [1], [2]. As one of the most important production equipment in manufacturing industry, assembly equipment stands out as pivotal machinery, enhancing both workpiece assembly efficiency and quality [3].

The robustness and accuracy of the controllers are important indicators for automatic assembly equipment. In manufacturing, high-precision position control is often based on the permanent magnet synchronous motor (PMSM) [4] for the servo systems. The automatic assembly equipment studied in this paper employs a position servo system driven by a servo motor coupled with a ball screw, which offers advantages such as good control performance and a simple structure. To better match the servo system with the mechanical system, proportional-integral-derivative (PID) controllers are often utilised for control system optimisation. However, traditional PID controllers may exhibit weak disturbance rejection capabilities. For complex and dynamic nonlinear servo systems [5], suboptimal PID parameters can result in subpar control performance, poor adaptability to varying operating conditions, and difficulty achieving higher precision in feed control. To address these issues, numerous advanced control methods have been proposed in the open literature; for instance, the fuzzy controller [6] is a popular one.

For the position servo system, nonlinear dynamics should be introduced into the controller design [7]. Nonlinear dynamics usually considers factors such as structural vibrations, external disturbances, and uncertainties of parameters [8]. To ensure the control robustness accuracy, researchers have proposed many methods [9], [10], including the nonlinear PID, fuzzy control, sliding mode control, model predictive control, iterative learning control, etc. The nonlinear PID controller is the first to address the nonlinear terms of the servo systems [11]. Matsukuma Fujiwara, Namba, and Ishida [12] considered a nonlinear PID control approach tailored for pneumatic servo systems and demonstrated superior performance and effective disturbance rejection. However, optimising the model parameters in nonlinear PID increases the difficulty in industrial applications [13]. To solve this problem, fuzzy logic is employed for adaptive tuning of nonlinear parameters [14]. Shahnazi, Shanechi, and Pariz [15] proposed an adaptive fuzzy PI sliding mode controller to effectively reduce control chattering and enhance control stability. Mu, Goto, Shibata, and Yamamoto [16] proposed a novel predictive fuzzy neural network method for the control of the position of the pneumatic servo system. The method constructs a hypothetical controlled object model by introducing an artificial neural network and uses a predictive fuzzy model to predict the model output. Bhimte, Bhole-Ingale, Shah, and Sekhar [17] designed a fractional order fuzzy PID controller to improve the position control of a rotary servo system.

Actually, fuzzy controllers have been widely used in various control applications [18], [19]. Common fuzzy controller structures include the traditional fuzzy controller

Manuscript received 9 March, 2024; accepted 16 May, 2024.
This research was supported by the National Natural Science Foundation of China under Grant No. 51975568.

and the hybrid fuzzy controller [20]. The hybrid controller integrates fuzzy logic with other intelligent algorithms, such as fuzzy PID control, fuzzy sliding mode control, fuzzy neural network control, and fuzzy control with evolution optimisers, etc. Meza, Santibanez, Soto, and Llama [21] presented a fuzzy PID controller for robot manipulators. Mani, Rajan, Shanmugam, and Joo [22] proposed a fractional fuzzy sliding mode control for PMSM. Nguyen *et al.* [23] developed a fuzzy neural network control for brain emotional learning. Furthermore, evolution optimisers are introduced into the fuzzy control and this type of hybrid fuzzy strategy currently becomes a hot research topic [24]. For example, Chen, Li, Zhang, and Li [25] used the ant colony algorithm to optimise the fuzzy PID controller. Mustafa Wang, and Tian [26] and Sathish Kumar, Naveen, Vijayakumar, Suresh, Asary, Madhu, and Palani [27] applied particle swarm optimisation to the fuzzy logic controller. The review of the literature indicates that evolution optimisers are able to produce the proper structures of fuzzy controllers to improve control performance.

However, although existing fuzzy control has improved the positioning accuracy of servo systems, some problems still remain. First, most control methods are designed and effective for specific controlled objects, while most of the nonlinear systems are different in properties and modelling. Second, the control performance of the system can be greatly affected by frictional disturbances and external disturbances of the loading condition of the objects. Hence, it is necessary to construct new fuzzy controllers for the automatic assembly equipment. However, very little work has been done to address these challenges in automatic assembly equipment. To bridge this research gap, a variable universe fuzzy PI controller based on the sparrow search algorithm (SSA-VUFPI) is proposed for servo system position control in automatic assembly equipment. The experimental test demonstrates good performance of the proposed method on some existing controllers by a shorter adjustment time, a smaller overshoot, and higher steady-state precision.

II. Ethics of the Proposed SSA-VUFPI Method

A. Mathematical Model of the Servo System

Figure 1 shows the structure of the automatic assembly device studied in this paper. The automatic clamping mechanism is responsible for clamping the workpieces at both ends; the robotic arm measurement system is responsible for measuring the axial deviation angle and centroid coordinates of the workpieces at both ends; the two-dimensional turntable is responsible for adjusting the axis of the workpiece to align the axial lines at both ends; the alignment mechanism consisting of the second and fourth axes aligns the centroids of the workpieces through movements in the X and Z directions; the pressing motion mechanism consisting of the first and third axes presses the workpiece through movements in the Y direction.

The centering and pressing work of the automatic assembly equipment is mainly realised by the position servo system by controlling the position and speed of the moving parts. Position servo systems drive motors and mechanical transmission units by means of control quantities transformed from input commands, and control the movement of each feed axis to the specified coordinates smoothly and accurately, so their performance plays an important role in assembly quality and work efficiency.

The position servo system includes key components such as the servo motor, ball screw, guideway, table, and measuring system. The control system converts commands into voltage signals, which are amplified and shaped to control the rotation of the servo motor and finally converted into a linear motion of the alignment platform through the coupling and the ball screw.

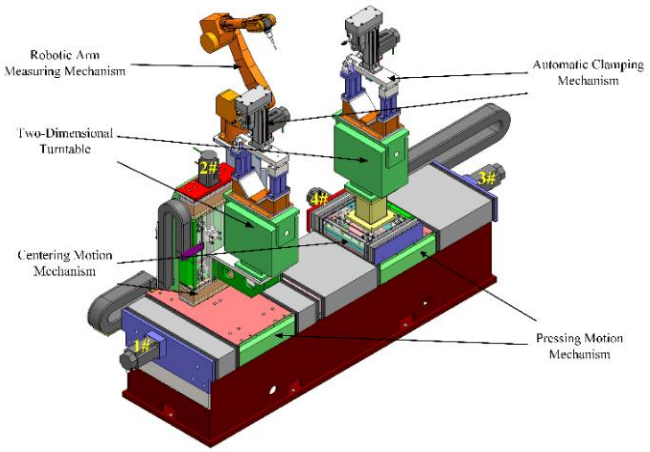

Fig. 1. The structure of the automatic assembly equipment.

The PMSM mathematical model in the rotation coordinates of the *d-q* axis is expressed as:

$$\begin{cases} u_d = Ri_d + \dfrac{\mathrm{d}}{\mathrm{d}t}\varphi_d - \omega_e\varphi_q, \\ u_q = Ri_q + \dfrac{\mathrm{d}}{\mathrm{d}t}\varphi_q - \omega_e\varphi_d, \end{cases} \tag{1}$$

where u_d, u_q and i_d, i_q are the stator voltage and current components on the *d-q* axis, respectively, ω_e is the electrical angular velocity of the rotor, R is the winding voltage of the stator, and φ_d, φ_q are the components of the magnetic chain of the stator on the *d-q* axis, expressed by:

$$\begin{cases} \varphi_d = L_d i_d + \varphi_f, \\ \varphi_q = L_q i_q, \end{cases} \tag{2}$$

where L_d and L_q are the inductance components on the *d-q* axes and φ_f is the magnetic chain of the permanent magnet.

Electromagnetic torque current and motion equations are described as:

$$T_e = \frac{3}{2}P_n[\varphi_f i_q + (L_d - L_q)i_d i_q], \tag{3}$$

$$T_e = T_L + D\omega_m + JP\omega_m, \tag{4}$$

where T_L is the load torque, ω_m is the motor angular speed, D is the viscous coefficient, and J is the moment of inertia. There is a coupling effect between ω_m, i_d, and i_q, which defines the nonlinear nature of the PMSM model.

To facilitate the design of the controller, (5) can be obtained by substituting (2) into (1) to decouple the PMSM:

$$\begin{cases} u_d = Ri_d + L_d \dfrac{\mathrm{d}}{\mathrm{d}t} i_d - \omega_e L_q i_q, \\ u_q = Ri_q + L_q \dfrac{\mathrm{d}}{\mathrm{d}t} i_q + \omega_e (L_d i_d + \varphi_f). \end{cases} \tag{5}$$

The position servo system generally adopts a three-loop control structure, including the current loop, speed loop, and position loop, as shown in Fig. 2, where a space vector pulse width modulation (SVPWM) is used in the control system. The current loop measures the current feedback, and the speed loop and position loop obtain their corresponding feedback signals by measuring and calculating the pulse signals from the encoder.

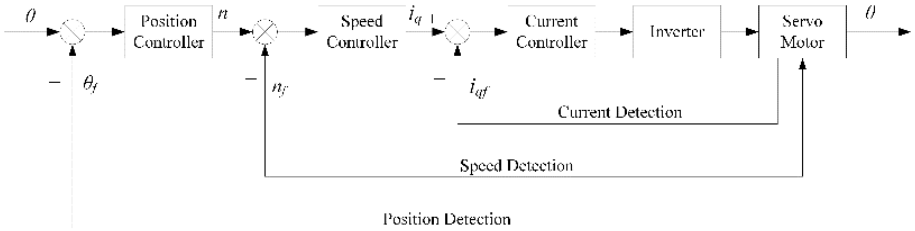

Fig. 2. Model of the position servo system.

B. Design of the SSA-VUFPI Controller

Traditional fuzzy PI control involves adding the fuzzy rule base on top of the PI controller, which dynamically adjusts the PI parameters in real time based on data from the rule base. With a predefined fuzzy rule base, the input error and its rate of change are fed into the rule base for fuzzy inference, allowing real-time adjustments to the two parameters (k_p, k_i) of the PI controller. Fuzzy controllers exhibit good robustness and simplicity in operation, but heavily rely on expert knowledge. Within a certain universe range, an excessive number of control rules not only increases the complexity of the system while ensuring precise system output, but also poses challenges. Conversely, too few rules may simplify the system but lead to suboptimal output performance.

The variable universe fuzzy PI control builds upon this by introducing adaptive adjustments to the universe of the fuzzy controller using the contraction-expansion (C-E) factors, thus correcting the drawback of excessive dependence on the initial universe in fuzzy control. The principle of a variable universe under the action of C-E factors is illustrated in Fig. 3, where α represents the C-E factors, and [−E, E] denotes the universe of fuzzy control. As the input quantity of the controller increases or decreases, the C-E factors change accordingly to dynamically control the contraction and expansion of the universe. The variable universe approach enhances the precision of the controller without altering the number of control rules.

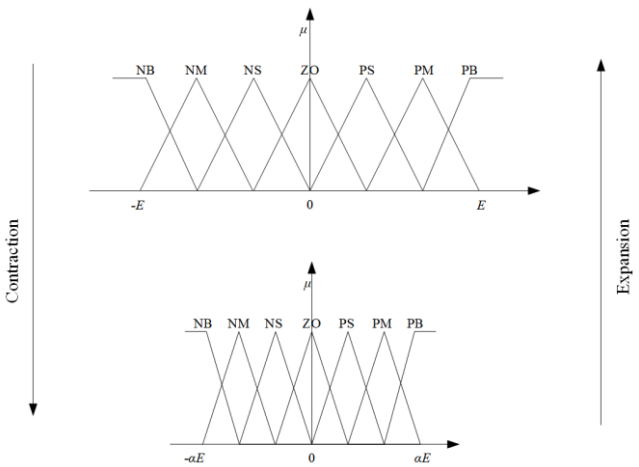

Fig. 3. The principle of a variable universe.

In a dual-input control system, both the input variable deviation e and the deviation rate of the variable e_c act on the scaling factor. The C-E factors have a significant impact on the entire variable universe system. The definition of the universe for input and output quantities is given in (6):

$$\begin{cases} X_e = [-\alpha(e)E, \alpha(e)E], \\ X_{e_c} = [-\beta(e_c)E_c, \beta(e_c)E_c], \end{cases} \tag{6}$$

where α, β are the C-E factors for the deviation of the input variable e and the deviation change rate e_c, respectively, $[-E, E]$ and $[-E_c, E_c]$ are the initial universes for each. The fuzzy linguistic variables in this context are set as {NB, NM, NS, ZO, PS, PM, PB}. C-E factors are typically designed on the basis of a function, and the expression is as follows:

$$\begin{cases} \alpha(x) = 1 - \rho e^{-\frac{kx^2}{2}}, \qquad \rho \in (0,1) \;\; k > 0, \\ \beta(y) = k_c \sum_{i=1}^{n} p_i \int_0^t e_i(\tau) dt + \beta(0), \quad \beta(0) = 1. \end{cases} \tag{7}$$

Due to the objective of the system of minimising error to zero, it is evident that the rate of change of the C-E factor is directly proportional to the variable deviation. However, (7) involves multiple parameters, making it challenging to determine the optimal values. Therefore, in this paper, the sparrow search algorithm (SSA) will be used directly to optimise the C-E factors.

SSA [28] is inspired by the biological characteristics of sparrows. The position of each sparrow represents a feasible solution within the specified search range during the optimisation. Assuming that the whole sparrow population size is n and the dimension of the problem is d, the whole sparrow population X can be expressed as

$$X = \begin{bmatrix} x_1^1 & x_1^2 & \cdots & x_1^d \\ x_2^1 & x_2^2 & \cdots & x_2^d \\ \vdots & \vdots & \ddots & \vdots \\ x_n^1 & x_n^2 & \cdots & x_n^d \end{bmatrix}. \tag{8}$$

The fitness values for all sparrows F_x are

$$F_x = \begin{bmatrix} f([x_1^1 & x_1^2 & \cdots & x_1^d]) \\ f([x_2^1 & x_2^2 & \cdots & x_2^d]) \\ \vdots & \vdots & \ddots & \vdots \\ f([x_n^1 & x_n^2 & \cdots & x_n^d]) \end{bmatrix}. \quad (9)$$

In SSA, the discoverers are sparrows with better positions. In each optimisation iteration, the position update for the discoverers is given by

$$X_{k,j}^{t+1} = \begin{cases} X_{k,j} \cdot \exp(-\dfrac{k}{\alpha \cdot T_{\max}}), & R_2 < D, \\ X_{k,j} + Q \cdot \boldsymbol{L}, & R_2 \geqslant D, \end{cases} \quad (10)$$

where t is the current iteration number, $j = 1, 2, 3, ..., d$, $X_{k,j}$ is the position of the k[th] sparrow in the j[th] dimension, α is a random number, $T_{\max}$ is the maximum number of iterations or the maximum number of loops, R_2 is the warning value, D is the safety threshold, Q is the random number obeying the normal distribution, and $\boldsymbol{L}$ is the unit matrix of $1 \times d$.

By combining the SSA with the variable universe fuzzy PI control, a variable universe fuzzy PI controller model based on the SSA (SSA-VUFPI) is shown in Fig. 4.

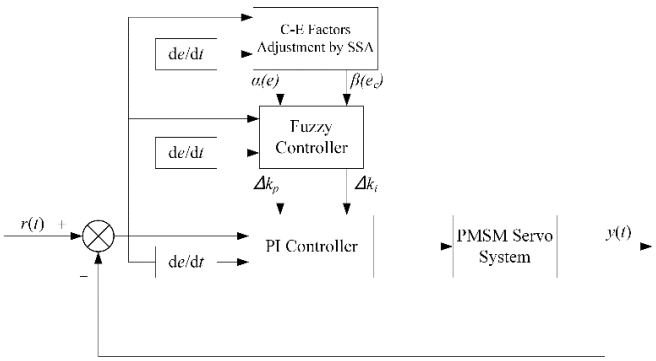

Fig. 4. SSA-VUFPI controller.

The algorithm dynamically adjusts the C-E factors according to the input variables and their rates of change. It further controls the real-time universe change of the fuzzy controller to output the most suitable PI change parameters (Δk_p, Δk_i), which are combined with the set PI base parameters (k_p, k_i) and passed into the controller to complete the optimisation. In this paper, the SSA-VUFPI control algorithm is applied to the outer loop position of a PMSM position servo control system to improve the dynamic performance and position control accuracy of the system.

The implementation of the proposed SSA-VUFPI is illustrated below.

Step 1: Set parameters, such as the size of the sparrow population, variable dimensions, maximum iteration count, and other parameters, for population initialisation.

Step 2: Randomly generate the sparrow population and define the objective fitness function.

Step 3: Calculate the fitness function value for each sparrow, and store the position information of the sparrow individual with the optimal fitness value.

Step 4: Update the position information of the sparrow individuals.

Step 5: Find the current best spatial position from the sparrow individuals.

Step 6: Check if the maximum iteration count has been reached; if not, go back to Step 4 for further updates. If the maximum iteration count is reached, proceed to the next step.

Step 7: Output the optimal solution for the variables, which represents the best C-E factors.

III. Simulation and Experiment Evaluation

A. Simulation Results

To evaluate the feasibility and effectiveness of the proposed controller, the position servo system is modelled and simulated by MATLAB/Simulink software, as shown in Fig. 5.

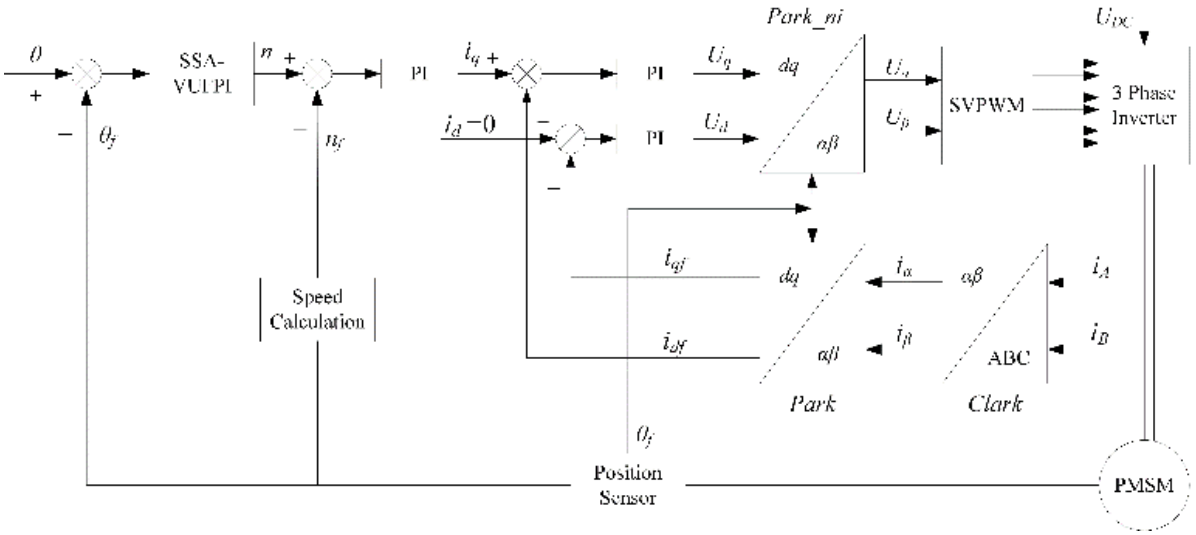

Fig. 5. Control block diagram of the position servo system based on SSA-VUFPI.

The simulation parameters in the model are as follows: the servo motor power is 750 W, the inductance value L is 7.55 × 10^{-3} H, the resistance value R is 1.34 Ω, the moment of inertia J is 0.193 × 10^{-3} kg×m^2, the damping factor B is 0. 008 Nm·s, the permanent magnetic flux φ_f is 0. 108 Wb, and the magnetic pole pair number p_n = 4.

In the SSA algorithm, the population size is set N to 20, the maximum number of iterations $T_{\max}$ is 10, the dimension of

the variable d to be solved four, and the optimisation variables α_e, α_{ec}, β_{Kp}, and β_{Ki} are the C-E factors of e, e_c, K_p, and K_i, respectively. The number of discoverers is $0.7N$, the number of alerts is taken as $0.2N$, the number of participants is taken as $0.1N$, and the prewarning value is taken as 0.6. Meanwhile, the integrated time absolute error (ITAE) of the error integration criterion is chosen as the fitness function. The expression of the ITAE indicator is

$$\text{ITAE}: s = \int_0^{\infty} t\,|\,e(t)\,|\,\mathrm{d}t, \tag{11}$$

where $e(t)$ is the deviation between the actual value and the set value and t is the optimisation time.

To further validate the superiority of the SSA-VUFPI controller in the control of PMSM servo systems, simulation experiments were conducted on the established position servo system model using the PI, VUFPI, and SSA-VUFPI controllers.

When the step signal is input to the system, the output curve of the system is shown in Fig. 6. The performance index of the controlled system under the action of the three controllers is shown in Table I.

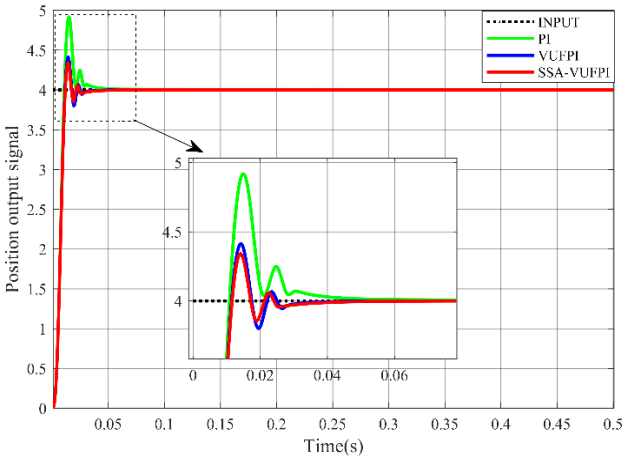

Fig. 6. Step response curves of three control systems.

TABLE I. THE PERFORMANCE INDICATORS OF THREE CONTROLLERS.

Controller	Steady-state error (rad)	Rise time (s)	Regulation time (s)	Overshoot (%)
PI	0.00877	0.01004	0.02721	22.9638
VUFPI	0.00134	0.01037	0.02125	10.3288
SSA-VUFPI	0.00022	0.01145	0.02024	8.5182

Analysing Fig. 6 and Table I, it can be seen that the system under the traditional PI controller has a larger overshoot and longer regulation time. The overshoot and regulation time of the system can be effectively reduced by the VUFPI. Although the rise time of the servo system controlled by the SSA-VUFPI is slightly longer than that of the other two controllers, the steady-state error, overshooting amount, and regulation time are better than that of the PI and VUFPI controllers.

Position servo systems are often affected by external factors during operation, which adversely affects the stability of the servo system. Therefore, simulation analysis was conducted on the disturbance rejection performance of the three controllers. At the 0.25 s time point, an external disturbance of 10 N·m was applied to the system. The anti-disturbance curves of three controllers are shown in Fig. 7. All three controllers exhibited dynamic disturbance responses, with the SSA-VUFPI controller demonstrating smaller overshoot and better stability. This indicates that the SSA-VUFPI controller possesses superior disturbance rejection capabilities and robustness.

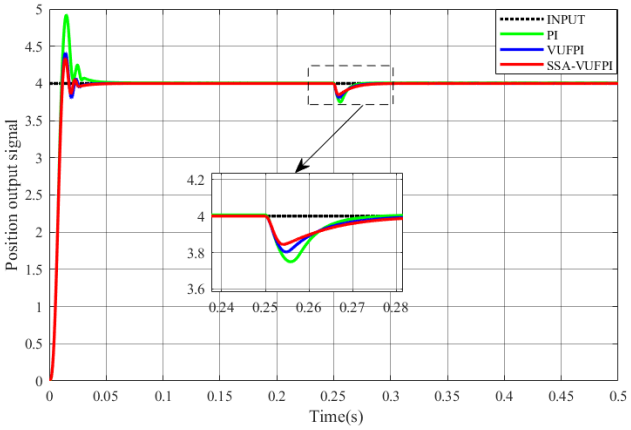

Fig. 7. Anti-disturbance curves of three controllers.

Meanwhile, to further compare the effect of the algorithm of this paper with other PID controllers in the PMSM servo system, the back propagation neural network PID (BP-PID), fractional-order PID (FOPID), and optimised PID based on the sparrow search algorithm (SSA-PID) are used to carry out simulation experiments and compared to the algorithm of this paper, respectively.

Under the same step signal, the output curve of the system is shown in Fig. 8. The performance index of the controlled system under the action of the three controllers is shown in Table II.

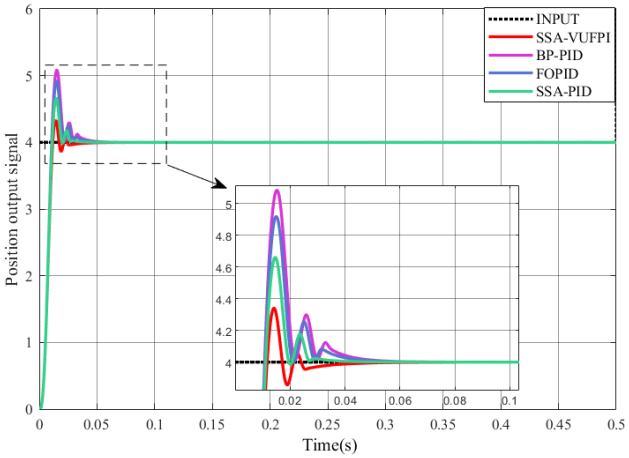

Fig. 8. Step response curves of four PID controllers.

TABLE II. THE PERFORMANCE INDICATORS OF FOUR PID CONTROLLERS.

Controller	Steady-state error (rad)	Rise time (s)	Regulation time (s)	Overshoot (%)
BP-PID	0.00146	0.01075	0.02745	27.1203
FOPID	0.00186	0.01086	0.02627	22.9475
SSA-PID	0.00047	0.01113	0.01798	16.5198
SSA-VUFPI	0.00022	0.01145	0.02024	8.5182

From the analysis of Fig. 8 and Table II, it can be seen that compared with the commonly used BP-PID, FOPID, and

SSA-PID algorithms, the algorithm of this paper has the best performance in terms of steady-state error, overshooting amount, and is second only to SSA-PID in terms of regulating time, and has the longest rise time.

Similarly, to verify the anti-jamming performance of this paper's algorithm against other commonly used PID algorithms, a simulation experiment is performed by applying a 10 Nm external disturbance at 0.25 s to the system. The output curve of the system at this time is shown in Fig. 9. From Fig. 9, it can be seen that all the controllers have dynamic response performance and the SSA-VUFPI controller designed in this paper has less overshoot and shows better immunity to interference compared to the remaining three PID controllers, followed by the FOPID algorithm.

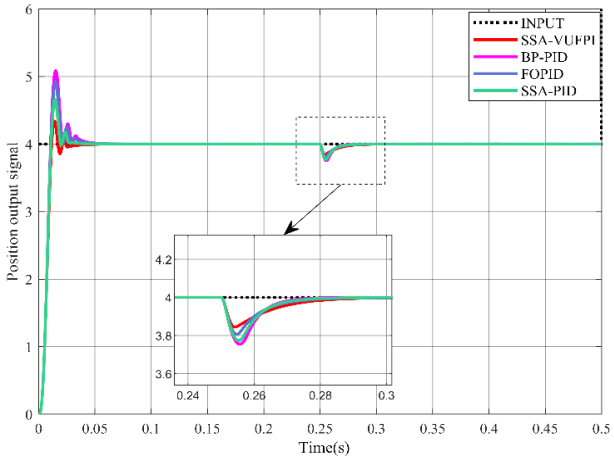

Fig. 9. Anti-disturbance curves of four PID controllers.

B. *Experimental Evaluation*

The automatic assembly system studied in this paper is shown in Fig. 10, which can perform high-precision alignment assembly of shaft and hole workpieces and monitor the assembly pressure during the assembly process. Its control system is mainly realised through the upper computer software and programmable logic controller (PLC), with the upper computer software designed in the C# programming language. To validate the practical performance of the control algorithm designed in this paper, the application of the control algorithm in the automated assembly system is achieved by invoking a dynamic link library (DLL) library generated from a simulation model in MATLAB through the upper computer software.

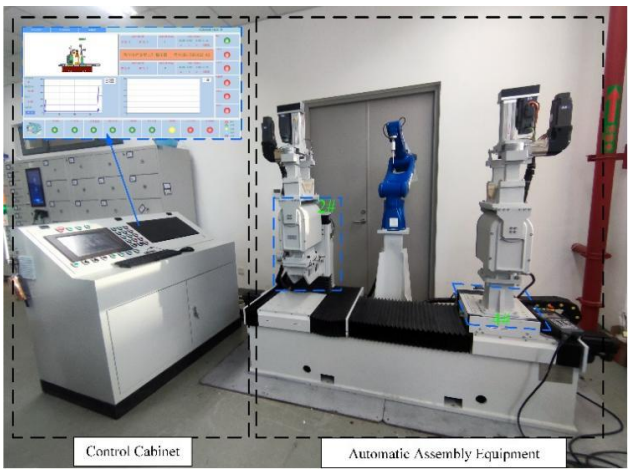

Fig. 10. Automatic assembly system.

After the SSA-VUFPI controller was incorporated into the automatic assembly system, the centering platform positioning accuracy experiment was carried out by adjusting the upper computer software. During the experiment, the workpiece is placed in a fixture and the YASKAWA-GP7 robotic arm, in conjunction with the Renishaw LP2 probe, is used to measure the coordinates of the workpiece centers at both ends. The deviation of the workpiece center at both ends is obtained, and after alignment adjustments using the second and fourth axes, the coordinates of the workpiece centers are measured again. The adjustment accuracy of the middle platform is determined by comparing the center deviations before and after alignment. Repeat the experiment by changing the initial coordinates of the workpiece at both ends for measurement. After conducting five repeated experiments, the center positioning accuracy before and after the controller is applied is as follows (Table III).

TABLE III. CENTER POSITIONING ACCURACY.

Controller	——		**SSA-VUFPI**	
Axis	2#	4#	2#	4#
Positional deviation (mm)	0.039	0.037	0.027	0.025
	0.034	0.036	0.019	0.029
	0.036	-0.037	0.032	0.031
	0.041	0.035	0.024	-0.025
	-0.037	0.048	0.027	0.028
Average deviation (mm)	0.0374	0.0386	0.0258	0.0276

Analysis of Table III reveals that under SSA-VUFPI control, the adjustment accuracy of Axis 2 has improved by 31.0 % compared to the original, and the adjustment accuracy of Axis 4 has increased by 28.5 %. This effectively improves the precision of workpiece alignment.

Taking a specific set of workpieces as an example, a press-fit experiment is conducted on the middle position servo system using SSA-VUFPI control to obtain the optimised force-displacement curve during the press-fit process. The quality of the press-fit is judged on the basis of the force-displacement curve. The schematic diagram of the press-fit process is illustrated in Fig. 11, where the press-fit force is obtained through the pressure sensor on the left. After conducting five repeated experiments for each system (before and after embedding the controller), the press-fit force curves for the workpiece are shown in Fig. 12.

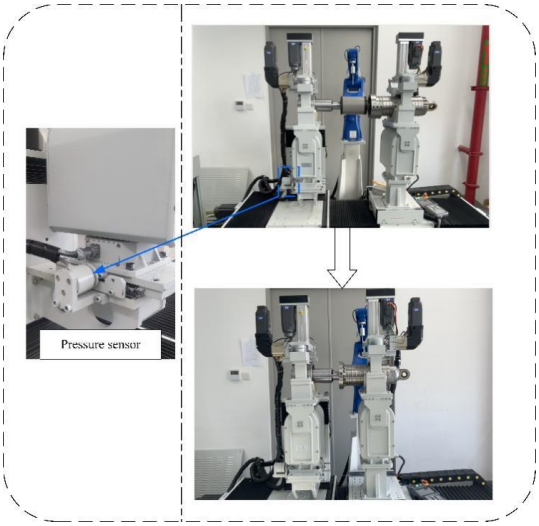

Fig. 11. The schematic diagram of the pressing process.

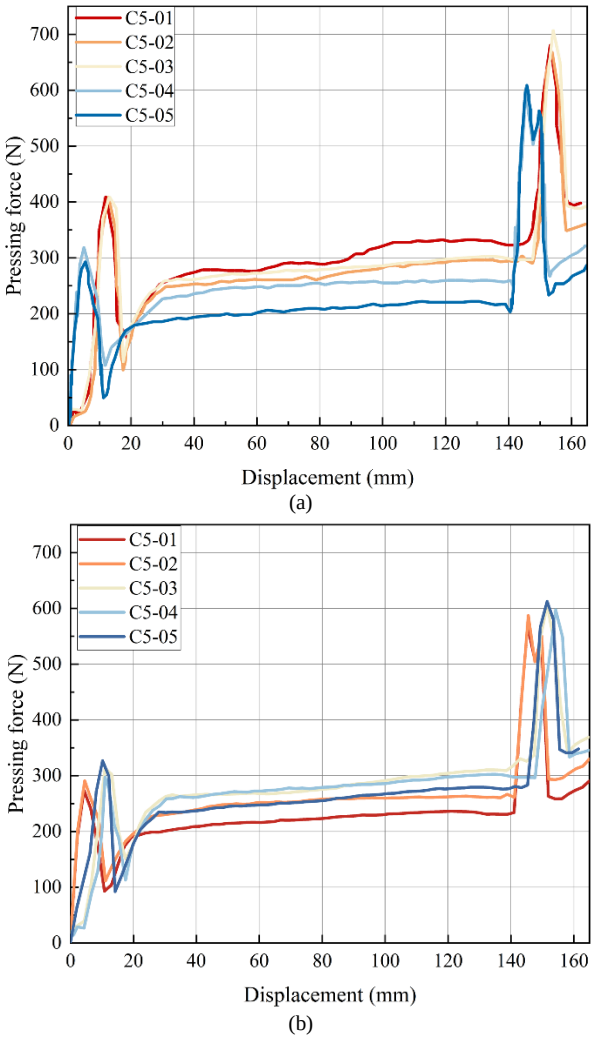

Fig. 12. Pressing force-displacement curve before and after optimisation: (a) Unoptimised pressing force-displacement curve; (b) Optimised pressing force-displacement curve.

The two peaks in the force curve represent the insertion processes of two sealing rings. From the analysis of Fig. 12, before introducing the SSA-VUFPI control, the maximum press-fit force for the first sealing ring insertion is 413.7 N, and for the second sealing ring, it is 707.6 N. After introducing SSA-VUFPI control, the maximum press-fit force for the first sealing ring insertion decreases by approximately 86.8 N, and for the second sealing ring, it decreases by about 95.1 N. At the same time, the fluctuation of the press force for repeated press-in of the same workpiece is smaller, and the change of the press force is smoother during the press-in process. Therefore, the SSA-VUFPI controlled position servo system can effectively improve centering accuracy, prevent seals from being damaged due to uneven force, and effectively improve assembly quality.

IV. CONCLUSIONS

To enhance the performance of the position servo system in the automatic assembly equipment and consequently elevate the quality of the workpiece assembly, an SSA-VUFPI control method is proposed. The SSA is used to optimise the fuzzy controller for the position loop control of the servo system. To validate the feasibility and efficacy of this proposed methodology, a position servo system simulation and experiment were carried out for centering. The main conclusions are as follows.

1. Compared with the traditional PI controller and the VUFPI controller, the SSA-VUFPI controller has smaller overshoot and steady-state error, shorter regulation time, and better disturbance resistance and robustness, where the overshoot is approximately 17.5 % lower than VUFPI and the steady-state error is 0.00112 rad lower.
2. The algorithm designed in this paper also has better performance compared to the currently used PID algorithms. The simulation results show that the SSA-VUFPI controller proposed in this paper is significantly better than the BP-PID, FOPID, and SSA-PID controllers, and the tracking characteristics, interference immunity, and robustness are significantly improved.
3. The SSA-VUFPI controller was used to control the position servo system for the positioning and assembly experiments of automatic assembly equipment, and the results showed that the positioning accuracy of the two axes controlled by this method was improved by 31.0 % and 28.5 %, respectively. During the assembly process, the maximum assembly force in the extrusion of the seal ring decreased by 86.8 N and 95.1 N, respectively, and the pressing force was smoother, effectively improving the quality of the assembly.

In this paper, the control for centering of automatic assembly equipment has been studied and some results have been obtained, but certain unresolved issues warrant further exploration. The follow-up work will continue to investigate the optimisation of the position servo system control performance.

CONFLICTS OF INTEREST

The authors declare that they have no conflicts of interest.

REFERENCES

[1] J. Jiang, Z. Huang, Z. Bi, X. Ma, and G. Yu, "State-of-the-Art control strategies for robotic PiH assembly", *Robotics and Computer-Integrated Manufacturing*, vol. 65, art. 101894, 2020. DOI: 10.1016/j.rcim.2019.101894.

[2] F. J. Abu-Dakka, B. Nemec, A. Kramberger, A. G. Buch, N. Krüger, and A. Ude, "Solving peg-in-hole tasks by human demonstration and exception strategies", *Industrial Robot*, vol. 41, no. 6, pp. 575–584, 2014. DOI: 10.1108/IR-07-2014-0363.

[3] D. E. Whitney, *The Potential Assembly Modeling in Product Development and Manufacturing*. Cambridge: MIT Press, 1996.

[4] A. M. O. Anwer, F. A. Omar, H. Bakir, and A. A. Kulaksiz, "Sensorless control of a PMSM drive using EKF for wide speed range supplied by MPPT based solar PV system", *Elektronika ir Elektrotechnika*, vol. 26, no. 1, pp. 32–39, 2020. DOI: 10.5755/j01.eie.26.1.25308.

[5] J. Yao, "Model-based nonlinear control of hydraulic servo systems: Challenges, developments and perspectives", *Frontiers of Mechanical Engineering*, vol. 13, pp. 179–210, 2018. DOI: 10.1007/s11465-018-0464-3.

[6] B. Y. Suprapto, S. Dwijayanti, and D. Amri, "Development of a position control system for wheeled humanoid robot movement using the swerve drive method based on fuzzy logic type-2", *Elektronika ir Elektrotechnika*, vol. 30, no. 1, pp. 4–13, 2024. DOI: 10.5755/j02.eie.35912.

[7] X. Zhao, X. Wang, L. Ma, and G. Zong, "Fuzzy approximation based asymptotic tracking control for a class of uncertain switched nonlinear systems", *IEEE Transactions on Fuzzy Systems*, vol. 28, no. 4, pp. 632–644, 2020. DOI: 10.1109/TFUZZ.2019.2912138.

[8] H. Yang, Z. Wang, T. Zhang, and F. Du, "A review on vibration analysis and control of machine tool feed drive systems", *The International Journal of Advanced Manufacturing Technology*, vol. 107, pp. 503–525, 2020. DOI: 10.1007/s00170-020-05041-2.

[9] F.-J. Lin, S.-G. Chen, and C.-W. Hsu, "Intelligent backstepping control using recurrent feature selection fuzzy neural network for synchronous

reluctance motor position servo drive system", *IEEE Transactions on Fuzzy Systems*, vol. 27, no. 3, pp. 413–427, 2019. DOI: 10.1109/TFUZZ.2018.2858749.

[10] W. Lu, B. Tang, K. Ji, K. Lu, D. Wang, and Z. Yu, "A new load adaptive identification method based on an improved sliding mode observer for PMSM position servo system", *IEEE Transactions on Power Electronics*, vol. 36, no. 3, pp. 3211–3223, 2021. DOI: 10.1109/TPEL.2020.3016713.

[11] C. Zhao and L. Guo, "PID controller design for second order nonlinear uncertain systems", *Science China Information Sciences*, vol. 60, art. no. 022201, pp. 1–13, 2017. DOI: 10.1007/s11432-016-0879-3.

[12] T. Matsukuma, A. Fujiwara, M. Namba, and Y. Ishida, "Non-linear PID controller using neural networks", in *Proc. of International Conference on Neural Networks (ICNN'97)*, 1997, pp. 811–814, vol. 2. DOI: 10.1109/ICNN.1997.616127.

[13] Y.-D. Son, S.-D. Bin, and G.-G. Jin, "Stability analysis of a nonlinear PID controller", *International Journal of Control, Automation and Systems*, vol. 19, pp. 3400–3408, 2021. DOI: 10.1007/s12555-020-0599-y.

[14] H. Chaoui and P. Sicard, "Adaptive fuzzy logic control of permanent magnet synchronous machines with nonlinear friction", *IEEE Transactions on Industrial Electronics*, vol. 59, no. 2, pp. 1123–1133, 2012. DOI: 10.1109/TIE.2011.2148678.

[15] R. Shahnazi, H. M. Shanechi, and N. Pariz, "Position control of induction and DC servomotors: A novel adaptive fuzzy PI sliding mode control", in *Proc. of 2006 IEEE Power Engineering Society General Meeting*, 2006, pp. 9–12.

[16] S. Mu, S. Goto, S. Shibata, and T. Yamamoto, "Intelligent position control for pneumatic servo system based on predictive fuzzy control", *Computers and Electrical Engineering*, vol. 75, pp. 112–122, 2019. DOI: 10.1016/j.compeleceng.2019.02.016.

[17] R. Bhimte, K. Bhole-Ingale, P. Shah, and R. Sekhar, "Precise position control of Quanser servomotor using fractional order fuzzy PID controller", in *Proc. of 2020 IEEE Bombay Section Signature Conference (IBSSC)*, 2020, pp. 58–63. DOI: 10.1109/IBSSC51096.2020.9332216.

[18] M. Neubauer, F. Brenner, C. Hinze, and A. Verl, "Cascaded sliding mode position control (SMC-PI) for an improved dynamic behavior of elastic feed drives", *International Journal of Machine Tools and Manufacture*, vol. 169, art. 103796, 2021. DOI: 10.1016/j.ijmachtools.2021.103796.

[19] Y. Sun, M. Yang, B. Wang, Y. Chen, and D. Xu, "Precise position control based on resonant controller and second-order sliding mode observer for PMSM-driven feed servo system", *IEEE Transactions on Transportation Electrification*, vol. 9, no. 1, pp. 196–209, 2023. DOI: 10.1109/TTE.2022.3182027.

[20] M. J. Er and S. Mandal, "A survey of adaptive fuzzy controllers: Nonlinearities and classifications", *IEEE Transactions on Fuzzy Systems*, vol. 24, no. 5, pp. 1095–1107, 2016. DOI: 10.1109/TFUZZ.2015.2501439.

[21] J. L. Meza, V. Santibanez, R. Soto, and M. A. Llama, "Fuzzy self-tuning PID semiglobal regulator for robot manipulators", *IEEE Transactions on Industrial Electronics*, vol. 59, no. 6, pp. 2709–2717, 2012. DOI: 10.1109/TIE.2011.2168789.

[22] P. Mani, R. Rajan, L. Shanmugam, and Y. H. Joo, "Adaptive fractional fuzzy integral sliding mode control for PMSM model", *IEEE Transactions on Fuzzy Systems*, vol. 27, no. 8, pp. 1674–1686, 2019. DOI: 10.1109/TFUZZ.2018.2886169.

[23] H. B. Nguyen *et al.*, "Fuzzy hybrid neural network control for uncertainty nonlinear systems based on enhancement search algorithm", *International Journal of Fuzzy Systems*, vol. 24, no. 8, pp. 3384–3402, 2022. DOI: 10.1007/s40815-022-01374-0.

[24] W. Li, G.-G. Wang, and A. H. Gandomi, "A survey of learning-based intelligent optimization algorithms", *Archives of Computational Methods in Engineering*, vol. 28, pp. 3781–3799, 2021. DOI: 10.1007/s11831-021-09562-1.

[25] G. Chen, Z. Li, Z. Zhang, and S. Li, "An improved ACO algorithm optimized fuzzy PID controller for load frequency control in multi area interconnected power systems", *IEEE Access*, vol. 8, pp. 6429–6447, 2020. DOI: 10.1109/ACCESS.2019.2960380.

[26] G. I. Y. Mustafa, H. P. Wang, and Y. Tian, "Vibration control of an active vehicle suspension systems using optimized model-free fuzzy logic controller based on time delay estimation", *Advances in Engineering Software*, vol. 127, pp. 141–149, 2019. DOI: 10.1016/j.advengsoft.2018.04.009.

[27] A. Sathish Kumar, S. Naveen, R. Vijayakumar, V. Suresh, A. R. Asary, S. Madhu, and K. Palani, "An intelligent fuzzy-particle swarm optimization supervisory-based control of robot manipulator for industrial welding applications", *Scientific Reports*, vol. 13, no. 1, art. no. 8253, 2023. DOI: 10.1038/s41598-023-35189-2.

[28] J. Xue and B. Shen, "A novel swarm intelligence optimization approach: Sparrow search algorithm", *Systems Science & Control Engineering*, vol. 8, no. 1, pp. 22–34, 2020. DOI: 10.1080/21642583.2019.1708830.